Computer simulations of a liquid crystalline dendrimer in liquid crystalline solvents

Mark R. Wilson,[a] Jaroslav M. Ilnytskyi, and Lorna M. Stimson
Department of Chemistry, University of Durham, South Road, Durham DH1 3LE, United Kingdom

(Received 16 April 2003; accepted 9 May 2003)

Molecular dynamics simulations have been carried out to study the structure of a model liquid crystalline dendrimer (LCDr) in solution. A simplified model is used for a third generation carbosilane LCDr in which united atom Lennard-Jones sites are used to represent all heavy atoms in the dendrimer with the exception of the terminal mesogenic groups, which are represented by Gay–Berne potentials. The model dendrimer is immersed in a mesogenic solvent composed of Gay–Berne particles, which can form nematic and smectic-A phases in addition to the isotropic liquid. Markedly different behavior results from simulations in the different phases, with the dendrimer changing shape from spherical to rodlike in moving from isotropic to nematic solvents. In the smectic-A phase the terminal mesogenic units are able to occupy five separate smectic layers. The change in structure of the dendrimer is mediated by conformational changes in the flexible chains, which link the terminal mesogenic moieties to the dendrimer core. © *2003 American Institute of Physics.* [DOI: 10.1063/1.1588292]

I. INTRODUCTION

There is considerable interest in the properties of new mesomorphic materials, which are composed of molecules with novel architectures. These include rod-coil molecules,[1] polyphilic molecules,[2] ternary block-copolymers,[3] and dendritic molecules.[4] In each of these systems it is possible to combine molecular segments containing mesogenic moieties with separate segments which contain flexible entities. It is also possible to combine molecular segments with radically different types of molecular interactions (for example, aliphatic, aromatic, fluoro, and siloxane-based segments) to induce microphase separation. The combination of rigidity/flexibility and microphase separation opens up a wide-variety of possibilities for new self-assembled structures and has led to a series of novel mesophase morphologies.[5]

In the case of liquid crystalline dendrimers (LCDr), there is the possibility of incorporating mesogenic groups into the body of the dendrimer, which can lead to the formation of calamitic nematic and smectic thermotropic phases.[6] Or alternatively, mesogenic groups can be bonded to the ''surface'' of a dendrimer.[7] The latter raises an interesting possibility. Conformational changes in the structure of the dendrimer could allow it to rearrange the distribution of terminal mesogenic groups. This provides a mechanism for formation of different types of mesophase. For example, with carbosilane LCDrs it has been suggested that the dendrimer can form rods leading to smectic-A phase formation; or form discs which can pack to form columns, leading in turn to the formation of columnar mesophases.[8]

There have been a number of previous studies of simple bead models for nonliquid crystalline dendrimers.[9–11] In this paper we carry out the first simulation of a liquid crystalline dendrimer in solution. A detailed model for a third generation carbosilane dendrimer is studied in the presence of a mesogenic solvent. We employ a hybrid model in which all heavy atoms in the nonmesogenic parts of the dendrimer are represented by Lennard-Jones sites, and both the mesogenic groups and the solvent are represented by anisotropic (Gay–Berne) sites. There is great interest in the structure of such dendrimers in solution, not least because they provide an insight into how the terminal mesogenic groups are able to order by rearrangement of the dendrimer structure. Moreover, LCDrs can be used in nematic liquid crystal phases (dendrimer filled nematics) to produce polarizer free liquid crystal displays,[12,13] which work by controlling light scattering. In this case, application of an electric field causes realignment of nematic domains within the structure, providing switching from a scattering to a transparent mode. Finally, solution studies of a LCDrs provide a first stage towards the simulation of bulk mesophases, and a more detailed understanding of the structures dendritic molecules adopt in the bulk.

The layout of this paper is as follows: The simulation model is described in Sec. II, results for the structure of the model dendrimer in isotropic, nematic, and smectic solvents are presented in Sec. III, finally we draw some conclusions in Sec. IV.

II. SIMULATION MODEL

A. Liquid crystalline dendrimer

The simulation model used is based on a *simplified structure* for a third generation carbosilane dendrimer. The chemical structure of the real dendrimer is shown in Fig. 1(a), and a schematic two-dimensional diagram is shown in Fig. 1(b) highlighting the silicon atom branching points, the connecting chains and the terminal mesogenic groups. In the

[a]Author to whom correspondence should be addressed; Electronic mail: mark.wilson@durham.ac.uk

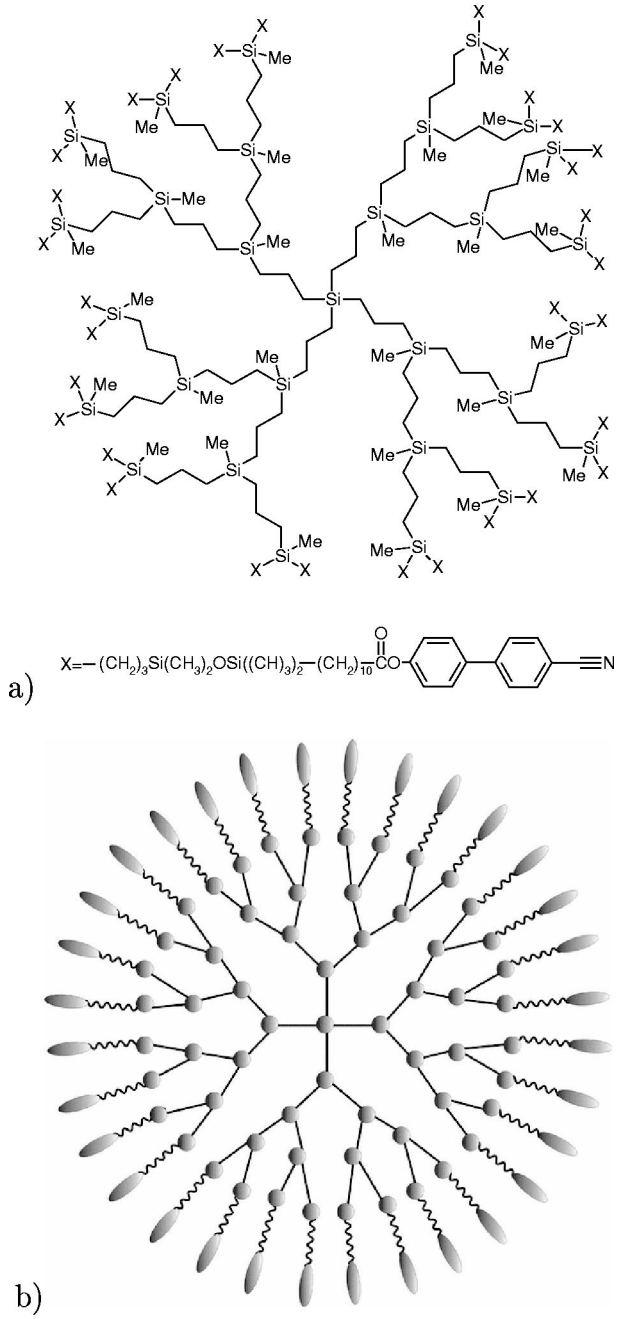

FIG. 1. (a) Chemical structure of a third generation carbosilane dendrimer; (b) schematic diagram showing only the branching points, connecting chains and 32 terminal mesogenic groups.

model dendrimer each of the 32 mesogenic groups is represented by a Gay–Berne (GB) potential.[14] Here the mesogenic group is chosen as the cyanobiphenyl unit plus the ester connecting group. In the rest of the dendrimer each heavy atom (silicon, carbon, and oxygen) is replaced by a single united atom Lennard-Jones site, which incorporates any hydrogens attached to these atoms. This gives a total of $N_{\mathrm{LJ}}^{(1)}=781$ LJ sites and $N_{\mathrm{GB}}^{(1)}=32$ GB sites in the model.

Building an initial stable nonoverlapping configuration for a complicated dendrimer is nontrivial. In this work, the backbone of the dendrimer was generated as a branched network using a simple geometric algorithm, to which hydrogens were added to complete the valency of each heavy atom. At the initial stage the mesogenic units were represented by a rigid rod of Lennard-Jones atoms. Monte Carlo simulations of this ''all-atom'' model were carried to eliminate close contacts and overlaps. We used the internal coordinate Monte Carlo program developed by one of the authors,[15] which proved particularly effective for this type of problem. When a relaxed conformation was reached the hydrogen atoms were stripped off, and each heavy atom was replaced by a single LJ site, and the rigid rods were replaced by GB sites.

Three types of nonbonded interactions are required: LJ–LJ, GB–GB, and LJ–GB. For the LJ sites, values of $\sigma_{\mathrm{LJ}}=3.93$ Å and $\epsilon_{\mathrm{LJ}}/k_B=47$ K (taken from Ref. 16) were used, which are appropriate for a united atom hydrocarbon model, and the cutoff distance for the potential was set to $r_{c,1}=9.8$ Å ($\equiv 2.5\sigma_{\mathrm{LJ}}$). For the GB sites we use the cut and shifted form of the potential studied by Brown and co-workers,[17] employing a length/breadth ratio $\kappa=3.5$ and a side-to-side/end-to-end well depth ratio of $\kappa'=5$. To scale to real units, values of $\sigma_{\mathrm{GB}}=3.829$ Å (estimated from the dimensions of the mesogenic unit) and $\epsilon_{\mathrm{GB}}/k_B=406.15$ K (from Ref. 18) were employed and the cutoff distance was set at $r_{c,2}=22$ Å ($\equiv 5.75\sigma_{\mathrm{GB}}$). The extended GB potential[19] was employed to describe the LJ–GB interactions. Here we used $\sigma_{\mathrm{LJ/GB}}=(\sigma_{\mathrm{GB}}^2+\sigma_{\mathrm{LJ}}^2)^{1/2}/\sqrt{2}\approx 3.88$ Å and $\epsilon_{\mathrm{LJ/GB}}/k_B=(\epsilon_{\mathrm{GB}}\epsilon_{\mathrm{LJ}})^{1/2}/k_B\approx 138.16$ K, with a cutoff distance of $r_{c,3}=16.5$ Å. All nonbonded potentials were shifted at the specified cutoff distances. The three cutoff distances were chosen to give approximately the same maximum numerical error for the potential at the cutoff (the maximum error corresponds to an end-to-end separation in the GB potential and at a point along the GB-axis vector in the LJ–GB interaction).

The intermolecular interactions are described by a simple harmonic force field of the form

$$E_{\mathrm{intra}}=\sum_{\mathrm{bonds}}\frac{k_{\mathrm{bond}}}{2}(l-l_{\mathrm{eq}})^2+\sum_{\mathrm{angles}}\frac{k_{\mathrm{angle}}}{2}(\theta-\theta_{\mathrm{eq}})^2+\sum_{\mathrm{dihedrals}}(a_{0,\mathrm{dih}}+a_{1,\mathrm{dih}}\cos\phi+a_{2,\mathrm{dih}}\cos^2\phi+a_{3,\mathrm{dih}}\cos^3\phi), \quad (1)$$

where the parameters take their usual meaning. In this work, we make use of the branched-alkane force field of Vlugt *et al.*[16] The force field is extended to the case of anisotropic sites, by adding an additional harmonic ''GB-angle'' interaction to keep the terminal GB sites parallel to the bonds joining them to the alkyl chain.[18] The full set of parameters used is summarized in Table I. Further details of this hybrid LJ/GB model can be found in our earlier work on liquid crystal dimers.[18]

B. Dendrimer in an LC solvent

The solvent systems were modeled by GB sites with the same parametrization as those of the LCDr end groups. Solvent simulations were started from a lattice containing 4732 solvent sites and equilibrated for 1 ns of time employing a timestep $\Delta t=3$ fs at fixed temperature $T=400$ K and different pressures. From this set of simulations we picked up

TABLE I. Summary of force field parameters used in this study.

Parameter	Value
Mass (GB)	$2.955\,7968\times10^{-25}$ kg
Moment of inertia	$0.273\,05\times10^{-23}$ kg m^{-2}
Mass (LJ)	$0.232\,4784\times10^{-25}$ kg
GB angle	0.0°
GB angle force constant	86.44×10^{-20} J rad^{-2}
$l_{\text{bond}}^{\text{LJ-LJ}}$	1.53 Å
$l_{\text{bond}}^{\text{LJ-GB}}$	7.46 Å
k_{bond}	361.291×10^{-20} J Å^{-2}
θ_{eq}	113°
k_{angle}	86.29×10^{-20} J rad^{-2}
a_0/k_B (nonbranched)	1009.728 K
a_1/k_B (nonbranched)	2018.466 K
a_2/k_B (nonbranched)	136.341 K
a_3/k_B (nonbranched)	−3164.52 K
a_0/k_B (branched)	1.394 K
a_1/k_B (branched)	2.787 K
a_2/k_B (branched)	0.188 K
a_3/k_B (branched)	−4.369 K

three final configurations with the reduced densities of $\rho^* = N^*(\sigma_0^{\text{GB}})^3/V = 0.231$, 0.2505, 0.2608, that correspond to the isotropic, nematic, and smectic-A phases, respectively. In our parametrization, the temperature of $T = 400$ K corresponds to the reduced temperature $T^* = k_B T/\epsilon_0^{\text{GB}} = 0.984$, and we found that the state points appear to be in very good agreement with the results of Ref. 17 where the phase diagrams for GB potentials with adjacent values of $\kappa = 3.4$ and $\kappa = 3.6$ have been studied.

The LCDr (as prepared in Sec. II A), was equilibrated initially in the gas phase using constant temperature molecular dynamics (MD) at 400 K (1 fs timestep), which yielded an isotropic arrangement of mesogenic groups. The isotropic LCDr was then placed in the three different solvents. Solvent/dendrimer overlaps were eliminated by removing any solvent molecules that directly overlapped with part of the dendrimer. As a result, the number of GB sites in the solvent dropped down to values of $N_{\text{GB}}^{(2)} = 4442$ (isotropic phase), $N_{\text{GB}}^{(2)} = 4441$ (nematic phase) and $N_{\text{GB}}^{(2)} = 4426$ (smectic-A phase). Finally, long (1 fs timestep) MD runs were performed for each mixture (1.0 ns isotropic phase −4.5 ns smectic-A phase), using the same constant temperature ($T = 400$ K) and pressure ($p = 0.018$, 0.021, 0.023 kg s^{-2} Å^{-1}) used in the original solvent equilibration.

In all simulations, the equations of motion were solved using a variant of the leap frog algorithm, which is suitable for both anisotropic and isotropic particles. The simulations employed the GBMOLDD program, which is a domain decomposition parallel molecular dynamics program developed by the authors. The basic program and algorithm used is described in Ref. 20 and the extension to the *NpT* ensemble is described in Ref. 21.

To monitor the orientational order in the mixture four uniaxial order parameters were introduced. The general formula

$$S = \langle P_2(\cos\theta_i)\rangle \tag{2}$$

applies to each, where θ_i is the angle between the long axis of the GB particle, $\mathbf{e}_i$, and the director. The latter is defined differently for each order parameter. For the total order parameter, S_{mix}, the average in Eq. (2) is performed over all $N_{\text{GB}}^{(1)} + N_{\text{GB}}^{(2)}$ sites with the director defined globally. S_{den} is measured for dendrimer GB sites only, using their own local director. S_{solv} is defined in the same way but by averaging over solvent GBs. Finally, $S_{d/s}$ is defined by averaging over all dendrimer GB sites, but measuring θ_i with respect to the director of the solvent.

III. RESULTS AND DISCUSSION

Figure 2 shows a sequence of three configurations taken from the equilibration run of the dendrimer in an isotropic solvent. As expected, the dendrimer adopts a spherical shape, with the alkyl chains wrapping around the core and the terminal mesogenic units arranged randomly near the surface of the dendrimer. Under good solvent conditions, we would expect the alkyl chains to be well-solvated by the Gay–Berne solvent molecules and the solvent to penetrate into some of the central regions of the dendrimer. However, the snapshots indicate that this is not the case. In Fig. 3 we compare the radius of gyration, R_g, of LJ sites for simulations in the gas phase and in the isotropic solvent. In the isotropic phase, after an initial equilibration period, the radius of gyration

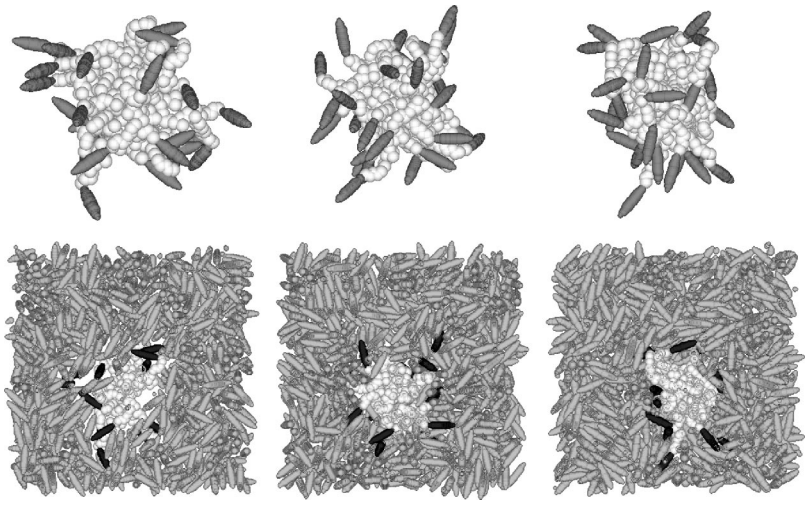

FIG. 2. Configurations showing the structure of the liquid crystal dendrimer on mixing with the isotropic solvent at $t = 0.1$, 0.15, 0.2 ns. Slices through the simulation box are shown below snapshots of the dendrimer with solvent particles removed.

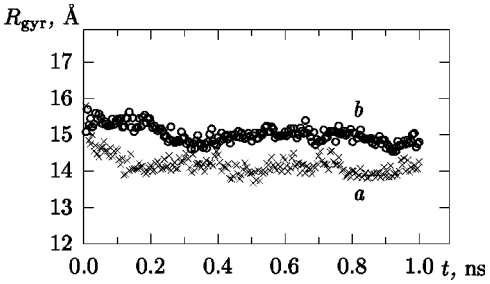

FIG. 3. The radius of gyration, R_g, plotted for the dendrimer in the gas phase (crosses) and in the isotropic solvent (circles).

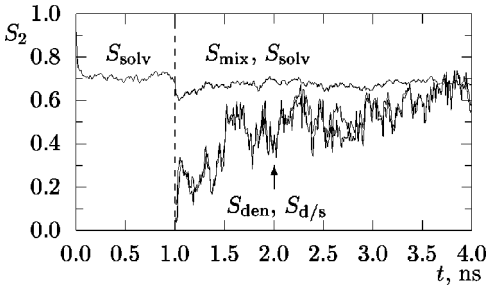

FIG. 5. The time dependence of the global system order parameter, S_{mix}, local solvent order parameter, S_{solv}, local LCDr order parameter, S_{den} and the order parameter of the LCDr with respect to the solvent, $S_{d/s}$, during the *NpT* simulations in the nematic solvent.

converges and fluctuates about a mean value of 14.9 Å (5.7% larger than the value in the gas phase), indicating only a small amount of solvent penetration into the interior of the dendrimer. The strength of GB–GB interactions means that the GB potential effectively acts as a *poor solvent* for the LJ parts of the LCDr. The terminal GB sites are therefore excluded from the globular center of the dendrimer but remain in intimate contact with the surrounding solvent. In the nematic and smectic phases the dendrimer contracts slightly, with the radius of gyration falling to 14.15 Å in the nematic and 13.95 Å in the smectic phase, suggesting that the alkyl chains are wrapped more tightly around the core in these solvents. The relatively rapid fluctuations in R_g about the mean value are caused by conformational changes in the alkyl chains surrounding the core. It is these conformational changes that lead to changes in dendrimer structure in different solvents (see below).

It is interesting to compare Fig. 2 with similar snapshots taken from the simulation in the nematic solvent (Fig. 4). In the nematic phase a structural change occurs in the LCDr over the course of 4 ns, the dendrimer core adapts a similar structure to the isotropic phase but the terminal mesogenic units align to lie close to the solvent director. This occurs through a rearrangement of alkyl chain conformations (see discussion below) resulting in the dendrimer forming a rod shape. The process of alignment is shown through the series of order parameters plotted in Fig. 5. Initially, a small drop in the order of solvent, S_{solv}, is seen immediately after the dendrimer is immersed. After this, S_{solv}, recovers to its original value, and S_{den} and $S_{d/s}$ grow until both reach approximately the same value as S_{solv}, S_{mix}. The core of the dendrimer acts as a defect in the nematic but has only a minor (local) effect on the order of the solvent as a whole. It is interesting to note that the rod-shaped structures seen in the third snapshot of Fig. 4 have been postulated to be responsible for smectic-A phase formation in generation three carbosilane dendrimers with cyanobiphenyl terminal groups.[8] In that study x-ray measurements from bulk dendrimer mesophases show measured spacings consistent with layers of mesogenic groups sandwiched between a soft dendritic matrix. While no direct quantitative comparison is possible for the system studied here, the simulations lend weight to the LCDr packing models suggested elsewhere,[8,22] indicating that whole-scale rearrangement of the LCDr structure can be driven by changes in the ordering of mesogenic units. (In bulk phases, there is also an additional packing consideration, as discussed in the molecular theory of Vanakaras and Photinos.[23] In some dendrimer systems we might expect strong thermodynamic selection of conformations according to their packing efficiency, this could have the effect of enhancing shape transitions from sphere to rod in the bulk dendrimer.)

Figure 6 shows the change in orientational order as the dendrimer is immersed in the smectic-A phase. Slow growth of orientational order occurs over approximately 3 ns of

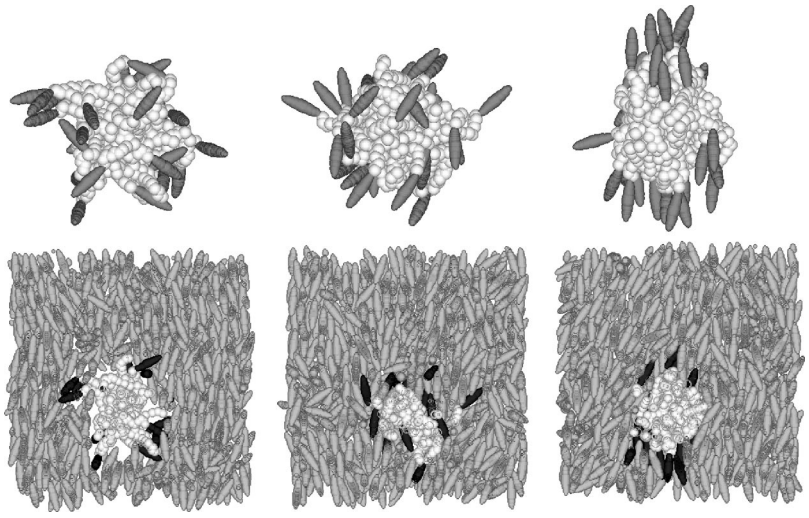

FIG. 4. Configurations showing the structure of the liquid crystal dendrimer on mixing with the nematic solvent at $t=1$, 2, 4 ns.

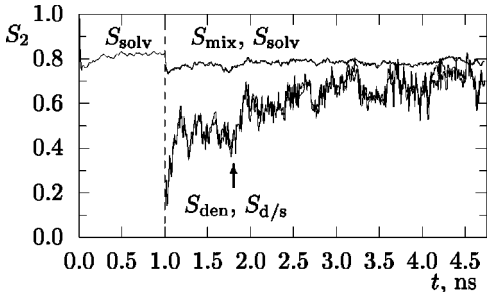

FIG. 6. The time dependence of the global system order parameter, S_{mix}, local solvent order parameter, S_{solv}, local LCDr order parameter, S_{den} and the order parameter of the LCDr with respect to the solvent, $S_{d/s}$, during the *NpT* simulations in the smectic-A solvent.

simulation. Thereafter the dendrimer order parameter fluctuates between values of $S_{\mathrm{den}} \approx S_{d/s} \approx 0.65-0.75$, which is slightly lower than the solvent order parameter S_{solv}. The snapshots in Fig. 7 show that major disruption is caused to the smectic layering close to the surface of the dendrimer, but within a distance of two/three molecular lengths from the dendrimer, the layers have recovered their undistorted form. It is interesting to note that the rod-shaped structure, seen in the nematic solvent, is not as pronounced in the smectic-A. This is because the mesogenic groups of the dendrimer are distributed over five separate smectic layers.

The radial distribution functions, $\rho(r)$ (averaged over all spatial directions) have been built for generation 2, generation 3, and the solvent; using the center of the dendrimer as the reference point for the plots. For the solvent we replaced each GB site by three adjacent spherical sites along the long axis of the former (this enhances the number density of the solvent allowing it to be displayed on the same scale at the LJ sites). For easy comparison the results for different solvents are presented in three separate plots in Fig. 8. Out to the branching point of generation 3, the dendrimer is relatively rigid so we get relatively narrow peaks corresponding to the united atoms in each generation. In contrast, the alkyl chains on the periphery of the dendrimer exhibit quite a broad distribution function. This arises because the chains are able to penetrate into the inner core of the dendrimer.

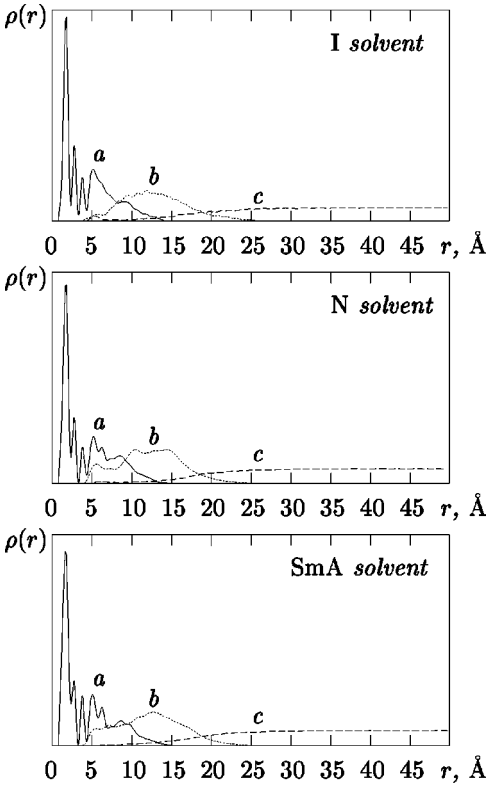

FIG. 8. The radial distribution function, $\rho(r)$ in arbitrary units averaged over all spatial directions for (a) atoms in the core (generations 1–3); (b) alkyl chain atoms; (c) the solvent. Plots for the dendrimer in the isotropic (*I*), nematic (N) and smectic-A (SmA) solvents are shown separately.

This is consistent both with earlier simulations of simpler dendrimer systems, and experimental work. Karatasos *et al.*[9] have carried out simulations of a bead–spring model dendrimer for generations 3–6. For beads in the outer shell of the G6 dendrimer, they notice considerable backfolding resulting with some beads appearing close to the core. Solid state rotational-echo double-resonance (REDOR) nuclear magnetic resonance (NMR) measurements for a flexible dendrimer provide similar evidence for backfolding.[24]

As noted in the snapshots, there is little penetration of

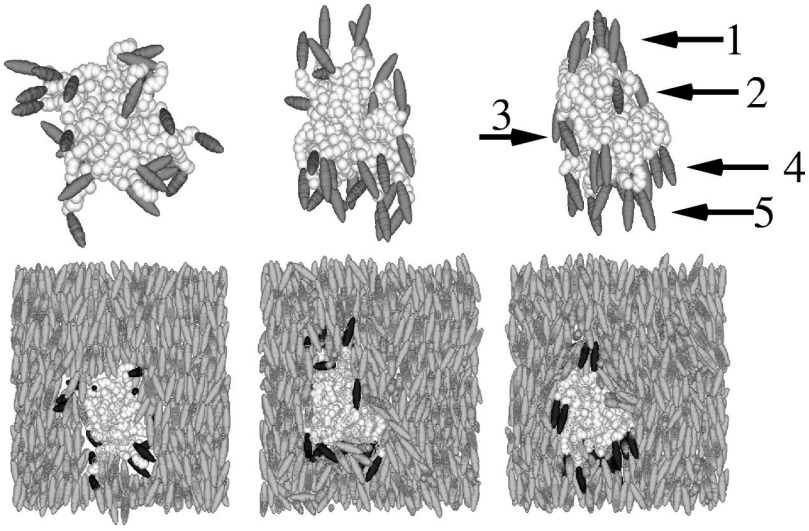

FIG. 7. Configurations showing the structure of the liquid crystal dendrimer on mixing with the smectic-A solvent at $t=1$, 2, 4 ns.

the solvent into the central core of the dendrimer. However, it is evident that Gay–Berne particles are able to penetrate some of the region occupied by the alkyl chains. This is probably due to instantaneous cavities that appear as a result of conformational changes in the alkyl chains as they wrap around the dendrimer core. Within statistical noise the differences between the radially averaged distributions for the three solvents are minimal.

The other question we would like to address concerns the isotropy of the dendrimer core in the cases of the nematic and smectic solvents. Particularly, we are interested whether or not the core is elongated in a direction collinear with the nematic director (which seems to be evident from the snapshots in Figs. 4 and 7). To answer this we calculated the partial radial distribution functions, $\rho_{\parallel}(r)$ within the conelike sectors limited by the angle $\theta=\pi/6$ around the head and tail directions of the nematic director, and $\rho_{\perp}(r)$, within the sector with the values for $\theta\in[\pi/3,2\pi/3]$ rad [θ corresponds to the polar angle in the spherical coordinates where the z axis ($\theta=0$) coincides with the nematic director]. The results are shown in Fig. 9 for different solvent phases. From these plots it is evident that there is significant anisotropy in the distribution of flexible alkyl chains in both nematic and smectic-A phases. In the nematic and smectic-A phases the chains tend to gather on the top and the bottom of the dendrimer core in a direction collinear with the nematic director. There is also a peak that develops at 9 Å in the $\rho_{\parallel}(r)$ plot for the third generation core within the nematic phase, which indicates some distortion of the outer part of the core along the nematic director. However, within statistical errors, the anisotropy in generation 2 is small. As expected, in both the nematic and smectic phases the solvent is able to penetrate further into the dendrimer in a direction perpendicular to the director. From these plots it seems likely that the chains fulfill the major role in allowing the LCDr to adapt its structure to best suit its environment. It seems highly plausible that a similar role is played in the bulk.

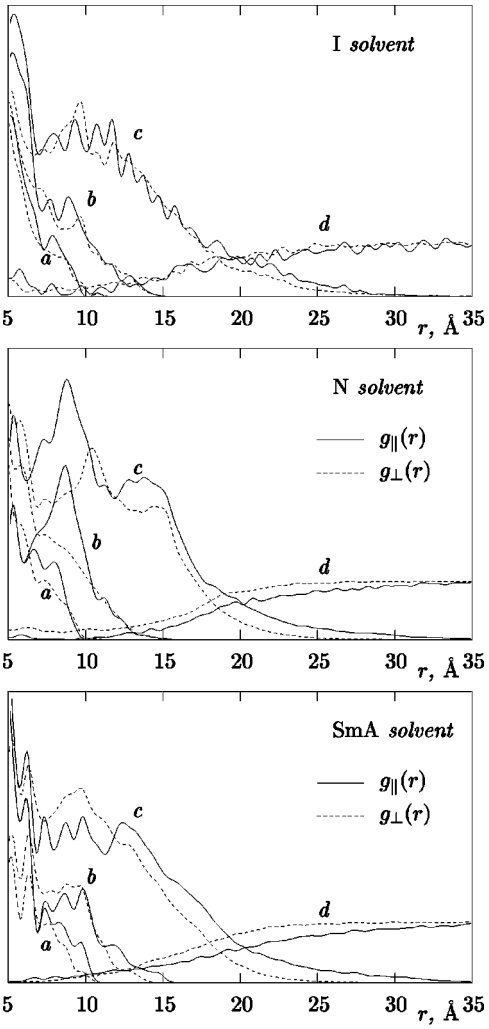

FIG. 9. The partial, angle dependent radial distribution functions $\rho_{\parallel}(r)$ (along the nematic director) and $\rho_{\perp}(r)$, perpendicular to it in arbitrary units for (a) all atoms within generation 2; (b) all atoms within generation 3; (c) all atoms within generation 3 and the alkyl chains; (d) the solvent. Plots for the dendrimer in the isotropic (I), nematic (N) and smectic-A (SmA) solvents are shown separately.

IV. CONCLUSIONS

We have carried out simulation studies of the structure of a model third generation liquid crystalline dendrimer in isotropic, nematic, and smectic-A solvents. We find the dendrimer core largely remains spherical in all three solvents, but that significant changes in shape occur for the rest of the molecule. These changes are facilitated by conformational fluctuations in the alkyl chains, which link the mesogenic groups to the core of the LCDr. They allow the dendrimer as a whole to become elongated along the nematic director and the terminal mesogenic groups to align with an order parameter approaching that of the solvent. The elongation of the LCDr to form rod-shaped structures is consistent with suggestions for how third generation carbosilane dendrimers pack within a bulk smectic phase. However, this can only be confirmed by a simulation of the bulk smectic phase itself, which at the current time remains computationally expensive for a model of the type studied here.

We find some penetration of the liquid crystal solvent into the region occupied by the alkyl chains but negligible penetration into the region occupied by the dendrimer core. However, the alkyl chains themselves are able to backfold and occupy some spaces within the core. This opens up possibilities for a simplified (coarse-grained) dendrimer model where the core is represented by a single (soft) spherical potential. The bulk phases of one such model are under investigation currently within our laboratory.

An interesting future extension to this work, could involve the addition of several more dendrimer molecules to the nematic solution to produce a dendrimer-filled nematic (DFN), which is believed to contain multiple poorly correlated liquid crystalline domains. The mesogenic solvent can then be coupled to an external field to directly simulate a DFN electro-optical switch. For some real DFN systems, the switching behavior can be quite complex with different switching regimes possible depending on the applied voltage; which suggests rearrangement in the dendrimer structure as seen in the current study.

ACKNOWLEDGMENTS

The authors wish to thank the UK EPSRC for funding High Performance Computers at the University of Durham to carry out this study, and for providing a PDRA for J.M.I. and a Ph.D. studentship for L.M.S.

[1] M. Lee, B. K. Cho, K. J. Ihn, W. K. Lee, N. K. Oh, and W. C. Zin, J. Am. Chem. Soc. **123**, 4647 (2001).
[2] S. Pensec, F. G. Tournilhac, P. Bassoul, and C. Durliat, J. Phys. Chem. B **28**, 3080 (1995).
[3] R. Stadler, C. Auschra, J. Beckmann, U. Krappe, I. Voigtmartin, and L. Leibler, Macromolecules **28**, 3080 (1995).
[4] V. Percec, W. D. Cho, and G. Ungar, J. Am. Chem. Soc. **122**, 10273 (2000).
[5] C. Tschierske, J. Mater. Chem. **11**, 2647 (2001).
[6] V. Percec, P. W. Chu, G. Ungar, and J. P. Zhou, J. Am. Chem. Soc. **117**, 11441 (1995).
[7] R. M. Richardson, S. A. Ponomarenko, N. I. Boiko, and V. P. Shibaev, Liq. Cryst. **26**, 101 (1999).
[8] S. A. Ponomarenko, N. I. Boiko, V. P. Shibaev, R. M. Richardson, I. J. Whitehouse, E. A. Rebrov, and A. M. Muzafarov, Macromolecules **33**, 5549 (2000).
[9] K. Karatasos, D. B. Adolf, and G. R. Davies, J. Chem. Phys. **115**, 5310 (2001).
[10] Z. Y. Chen and S. M. Cui, Macromolecules **29**, 7943 (1996).
[11] M. Murat and G. S. Grest, Macromolecules **29**, 1278 (1996).
[12] M. van Boxtel, D. Broer, C. Bastiaansen, M. Baars, and R. Janssen, Macromol. Symp. **154**, 25 (2000).
[13] M. W. P. L. Baars, M. C. W. van Boxtel, C. W. M. Bastiaansen, D. J. Broer, S. H. M. Sontjens, and E. W. Meijer, Adv. Mater. **12**, 715 (2000).
[14] J. G. Gay and B. J. Berne, J. Chem. Phys. **74**, 3316 (1981).
[15] M. R. Wilson, Liq. Cryst. **21**, 437 (1996).
[16] T. J. H. Vlugt, R. Krishna, and B. Smit, J. Phys. Chem. B **103**, 1102 (1999).
[17] J. T. Brown, M. P. Allen, E. M. del Rio, and E. de Miguel, Phys. Rev. E **57**, 6685 (1998).
[18] M. R. Wilson, J. Chem. Phys. **107**, 8654 (1997).
[19] D. J. Cleaver, C. M. Care, M. P. Allen, and M. P. Neal, Phys. Rev. E **54**, 559 (1996).
[20] J. M. Ilnytskyi and M. R. Wilson, Comput. Phys. Commun. **134**, 23 (2001).
[21] J. M. Ilnytskyi and M. R. Wilson, Comput. Phys. Commun. **148**, 43 (2002).
[22] M. W. P. L. Baars, S. H. M. Sontjens, H. M. Fischer, H. W. I. Peerlings, and E. W. Meijer, Chem.-Eur. J. **4**, 2456 (1998).
[23] A. G. Vanakaras and D. J. Photinos, J. Mater. Chem. **11**, 2832 (2001).
[24] K. L. Wooley, C. A. Klug, K. Tasaki, and J. Schaefer, J. Am. Chem. Soc. **119**, 53 (1997).